were transferred by vertical dipping at a surface pressure of 25 mN/m on a polyethylene terephthalate sheet precoated with five layers of cadmium icosanoate.[26]

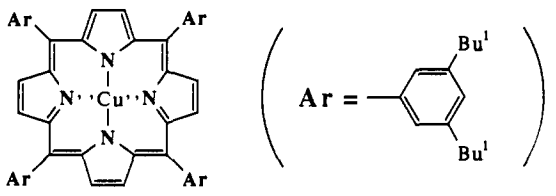

PM

We have employed ESR spectroscopy to determine the orientation of PM molecule in the mixed LB films. The hyperfine interaction of the unpaired 3d electron of copper(II) ion with its own nucleus causes the signal to split into four lines.[27] This hyperfine coupling as well as the g value are highly anisotropic for the planar copper(II) complexes: the hyperfine coupling constant is a factor of 10 smaller when the external magnetic field is perpendicular to the normal of the macrocycle plane ($A_\perp^{Cu} \approx 2 \times 10^{-3}$ cm^{-1}) compared with the parallel case ($A_\parallel^{Cu} \approx 2 \times 10^{-2}$ cm^{-1}). These features have been used to investigate the orientation of planar copper complexes in LB films.[28-31] The X-band ESR spectra were obtained with a Varian E-4 ESR spectrometer at room temperature.

A tilt of the macrocycle plane of PM with respect to the surface normal of the mixed LB film without n-alkane is consistent with the spectral data shown in Figure 1a. The hyperfine splitting due to copper is clearly observed in both of the spectra with the external magnetic field perpendicular ($H_\perp$) and parallel ($H_\parallel$) to the film surface. The $H_\perp$ spectrum shows a signal located at slightly higher field with a smaller coupling constant compared with the $H_\parallel$ spectrum. The angle between the normal of the macrocycle plane and that of the film surface is estimated to be around 50° by a preliminary simulation considering the distribution of tilt angles. The detail will be described elsewhere. The small peak located in the low-field region of the $H_\perp$ spectrum is assigned to disordered species.[29]

In contrast, the macrocycle plane of PM is almost perpendicular to the film surface in the LB film with hexatriacontane. The hyperfine splitting due to copper is clearly observed in the $H_\parallel$ spectrum, but not in the $H_\perp$ spectrum (Figure 1b). In the $H_\perp$ spectrum, the signal is almost a singlet with unresolved hyperfine structure. The g value of this signal is ca. 2.05, which is similar to the $g_\perp$ value of the ordinary copper porphyrins.[27]

These results show that hexatriacontane molecules can control the orientation of PM molecules in the mixed LB film. The mechanism involved in this process is not clear at present. These phenomena may be relevant to the case in which a long-chain n-alkane such as octadecane has been used to fill the vacancy in the hydrophobic portion to form a densely packed monolayer when the hydrophilic part of the amphiphilic molecule is larger than its hydrophobic part.[32-35]

The amount of hexatriacontane can be very small to control the orientation of PM in the mixed LB films. The value $r = 0.5$ is sufficient to obtain the oriented spectra similar to the ones shown in Figure 1b. This value corresponds to the 3/1 mixing of porphyrin and hexatriacontane, suggesting the importance of molecular interaction. The change in the orientation is already recognized at the value $r = 0.1$.

The structure of the mixed LB film depends on the chain length of n-alkane added in the films. Similar phenomena, although to a much lesser extent, have been observed in the ESR spectra of mixed LB films containing octadecane, the length being half that of hexatriacontane, with the molar ratio up to $r = 2$.

In this communication, we have shown a new way to control the orientation of dye molecules in LB films without any chemical modification. To our knowledge, the present example is the first case where a distinct orientational change has been obtained by adding a small amount of a molecule, the "trigger molecule", if we may call it, in LB films. This method will provide a new strategy for the fabrication of LB films with aimed structures and functions.

(26) Kuroda, S.; Sugi, M.; Iizima, S. *Thin Solid Films* **1983**, *99*, 21.
(27) Lin, W. C. In *The Porphyrins*; Dolphin, D., Ed.; Academic Press: New York, 1979; Vol. IV, p 355.
(28) Cook, M. J.; Daniel, M. F.; Dunn, A. J.; Gold, A. A.; Thomson, A. J. *J. Chem. Soc., Chem. Commun.* **1986**, 863.
(29) Cook, M. J.; Dunn, A. J.; Gold, A. A.; Thomson, A. J.; Daniel, M. F. *J. Chem. Soc., Dalton Trans.* **1988**, 1583.
(30) Pace, M. D.; Barger, W. R.; Snow, A. W. *Langmuir* **1989**, *5*, 973.
(31) Vandevyver, M.; Barraud, A.; Ruaudel-Teixier, A.; Maillard, P.; Gianotti, C. *J. Colloid Interface Sci.* **1982**, *85*, 571.
(32) Steiger, R.; Kitzing, R.; Junod, P. *J. Photogr. Sci.* **1973**, *21*, 107.
(33) Sotnikov, P. S.; Berzina, T. S.; Troitsky, V. I.; Valter, R. E.; Karlivan, G. A.; Neiland, O. YA. *Thin Solid Films* **1989**, *179*, 267.
(34) Kuhn, H. *Thin Solid Films* **1983**, *99*, 1.
(35) Shimidzu, T.; Iyoda, T.; Ando, M.; Ohtani, A.; Kaneko, T.; Honda, K. *Thin Solid Films* **1988**, *160*, 67.

Pure Absorption Gradient Enhanced Heteronuclear Single Quantum Correlation Spectroscopy with Improved Sensitivity

Lewis E. Kay,*,† Paul Keifer,‡ and Tim Saarinen‡

Protein Engineering Network Centres of Excellence and Departments of Medical Genetics, Biochemistry, and Chemistry, Medical Sciences Building University of Toronto Toronto, Ontario, Canada, M5S 1A8 Varian Associates, 3120 Hansen Way Palo Alto, California 94304

Received August 25, 1992

Recent advances in pulsed field gradient technology have led to the incorporation of pulsed field gradients in a large number of high-resolution NMR experiments.[1-5] While the advantages of including pulsed field gradients in NMR experiments are well documented in the literature,[6-8] a disadvantage with many of the published applications is the generation of spectra having undesirable mixed mode line shapes. Recently, schemes for recording pure absorption heteronuclear correlation spectra where the amplitude of one of the gradient pulses changes in alternate t_1 points have been suggested.[9-11] Because either N- or P-type coherence pathways, but not both, are selected with each scan, the theoretical signal-to-noise (S/N) ratios of peaks in such spectra are down by a factor of $(2)^{1/2}$ relative to (nongradient) pure absorption spectra recorded in the same amount of measuring time. In this communication, we describe a pulse sequence for recording pure absorption ^1H-^{15}N heteronuclear single quantum correlation (HSQC) spectra with coherence transfer selection achieved using gradients. This new method can offer sensitivity gains relative

† University of Toronto.
‡ Varian Associates.
(1) Hurd, R. E.; John, B. K. *J. Magn. Reson.* **1991**, *92*, 658.
(2) Vuister, G. W.; Boelens, R.; Kaptein, R.; Hurd, R. E.; John, B. K.; Van Zijl, P. C. M. *J. Am. Chem. Soc.* **1991**, *113*, 9688.
(3) Vuister, G. W.; Boelens, R.; Kaptein, R.; Burgering, M.; Van Zijl, P. C. M. *J. Biomol. NMR* **1992**, *2*, 301.
(4) John, B. K.; Plant, D.; Webb, P.; Hurd, R. E. *J. Magn. Reson.* **1992**, *98*, 200.
(5) Hurd, R. E.; John, B. K.; Plant, H. D. *J. Magn. Reson.* **1991**, *93*, 666.
(6) Hurd, R. E. *J. Magn. Reson.* **1990**, *87*, 422.
(7) Hurd, R. E.; John, B. K. *J. Magn. Reson.* **1991**, *91*, 648.
(8) Davis, A. L.; Laue, E. D.; Keller, J.; Moskau, D.; Lohman, J. *J. Magn. Reson.* **1991**, *94*, 637.
(9) Davis, A. L.; Keeler, J.; Laue, E. D.; Moskau, D. *J. Magn. Reson.* **1992**, *98*, 207.
(10) Tolman, J. R.; Chung, J.; Prestegard, J. P. *J. Magn. Reson.* **1992**, *98*, 462.
(11) Boyd, J.; Soffe, N.; John, B. K.; Plant, D.; Hurd, R. *J. Magn. Reson.* **1992**, *98*, 660.

0002-7863/92/1514-10663$03.00/0

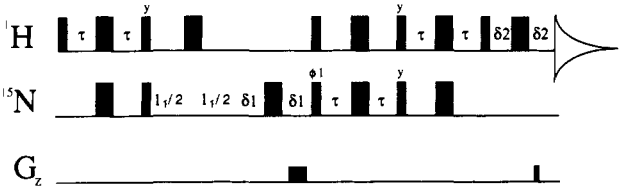

Figure 1. Pulse sequence of the sensitivity enhanced gradient ^{1}H–^{15}N HSQC experiment. Narrow pulses represent a flip angle of 90° with wider pulses representing a flip angle of 180°. Pulses for which the phases are not indicated are applied along the x axis. The delays τ, $\delta 1$, and $\delta 2$, are set to $1/(4J_{NH}) = 2.75$, 2.75, and 0.30 ms, respectively. The first gradient was applied with a strength of 30 G/cm and a duration of 2.5 ms, while the second gradient pulse of 29.05 G/cm was applied for 0.25 ms. Both gradient pulses are rectangular and are applied along the z axis. For each increment of t_1, the phases of the first ^{15}N 90° pulse and the receiver are inverted.[17] Decoupling is achieved with the use of the WALTZ decoupling sequence[18] using a 1-kHz radio frequency field. Water suppression is achieved solely with the use of the gradient pulses. The sequence can be shortened by elimination of the $\delta 2$ delays (and the ^{1}H 180° pulse in the middle). In this case, the first few points of the FID must be back predicted (after processing the F_1 dimension) using linear prediction[19] to eliminate the large phase distortion arising due to the finite duration of the second gradient pulse. Pure absorption spectra are obtained as described in the text.

to existing methods for moderately sized proteins.

Figure 1 illustrates the pulse sequence for recording ^{1}H–^{15}N gradient HSQC spectra with improved sensitivity. This sequence is very closely related to the family of sequences developed by Rance and co-workers[12,13] for obtaining sensitivity improvements in nongradient proton-detected heteronuclear correlation experiments. A straightforward calculation shows that, when $\phi_1 = \pm x$, the signal intensity for NH protons at the start of the acquisition period is given by

$$S(t_1,z) = \pm M_y \cos(\Theta_1) + M_x \sin(\Theta_1) \qquad (1)$$

where M_x and M_y are the x and y components of magnetization, respectively, and Θ_1 is given by $\Theta_1 = \omega_N t_1 + \gamma_N B^1(z)\tau^1 \pm \gamma_H B^2(z)\tau^2$, where ω_N is the Larmor frequency of the ^{15}N spin, γ_N and γ_H are the gyromagnetic ratios of ^{15}N and ^{1}H nuclei, respectively, $B^1(z)$ and $B^2(z)$ are the magnitudes of the z-dependent magnetic fields generated by the two gradient pulses, and τ^i (i = 1, 2) is the duration of a gradient pulse. In the derivation of eq 1 the effects of pulse imperfections and relaxation during the pulse sequence have been neglected. Refocusing of the effects of the gradients requires that $\tau^1/\tau^2 = \mp\gamma_H B^2(z)/\gamma_N B^1(z)$. For each t_1 value, two transients are recorded and stored separately, with the phase ϕ_1 incremented by 180° (from x to −x) and the amplitude of the second gradient pulse inverted for the second transient. Signals recorded for a given t_1 value and stored in separate memory locations are added and subtracted, a 90° zero-order phase correction is subsequently applied to every second FID, and the resultant data set is processed according to the STATES[14] recipe to yield a pure absorption spectrum with quadrature in F_1. A calculation of the signal intensities expected for NH protons in spectra recorded with the previously proposed pure absorption gradient HSQC schemes[9,11] shows that the enhanced gradient pulse sequence can be as much as a factor of 2 more sensitive, while a sensitivity gain is not expected for NH_2 groups. In addition, for NH peaks a theoretical enhancement of as much as a factor of $(2)^{1/2}$ is expected over the conventional ^{1}H–^{15}N HSQC spectrum.[15,16] In practice, the full sensitivity

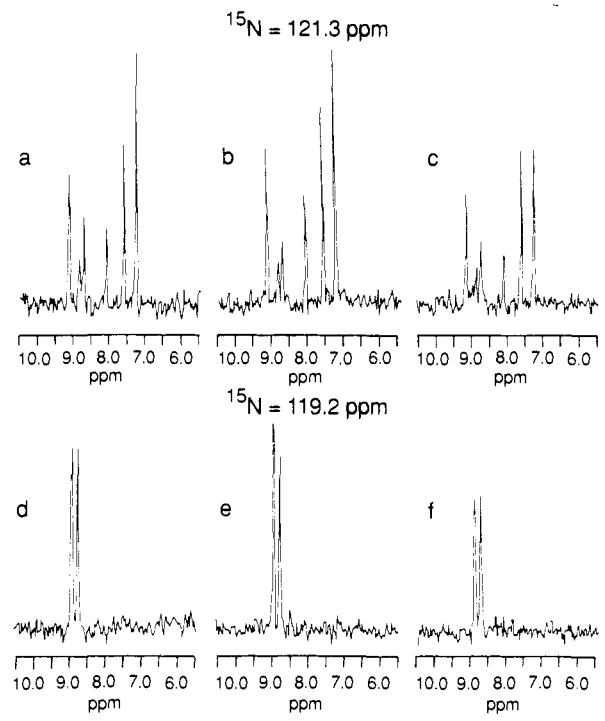

Figure 2. Cross sections from ^{1}H–^{15}N spectra of CBD recorded with different sequences: (a, d) nongradient, unenhanced HSQC sequence (two scans/FID, 28-Hz presaturation field); (b, e) enhanced gradient sequence of Figure 1 (one transient/FID); (c, f) gradient sequence of Davis et al.[9] (one transient/FID). The strengths and durations of the gradient pulses were identical in both gradient experiments. Spectra are normalized so that the noise level is the same in each spectrum.

enhancements are unlikely to be achieved due to the combined effects of the larger number of pulses in the enhanced sequence and relaxation losses that occur during the course of the various magnetization transfer steps.

Figure 2 illustrates cross sections at ^{15}N chemical shifts of 121.3 and 119.2 ppm from ^{1}H–^{15}N HSQC spectra recorded on the cellulose-binding domain fragment of a cellulase from *Cellulomonas fimi* (CBD), a protein fragment of 110 amino acids. The protein concentration was 1.7 mM in 90% H_2O, 10% D_2O, pH 6.0, and spectra were recorded at 30 °C on a Varian UNITY 500-MHz spectrometer. Figure 2a,d shows cross sections from spectra recorded using the standard (i.e., nongradient, unenhanced) HSQC sequence, with water suppression achieved using a 28-Hz presaturation field and a two-step phase cycle employed to suppress proton signals arising from protons not attached to ^{15}N nuclei. In Figures 2b,e and 2c,f the same cross sections from gradient spectra recorded with the sequences of Figure 1 and of Davis et al.,[9] respectively, are illustrated. In the case of the gradient spectra, only a single transient was recorded per FID, and water suppression and suppression of protons not attached to ^{15}N spins were achieved solely through the use of gradient pulses. An average sensitivity improvement of a factor of 1.40 ± 0.18 is obtained for NH peaks with the enhanced gradient sequence, while the average S/N ratio of the NH_2 peaks is lower by 11%. In addition, we have recorded a nongradient version of the enhanced sensitivity HSQC experiment with a two-step phase cycle to suppress protons not attached to ^{15}N and using a 28-Hz radio frequency field for presaturation (data not shown). Relative to the unenhanced, nongradient version of the HSQC experiment, an average S/N increase of 10% is obtained for the NH peaks. Thus, the gradient version of the enhanced sensitivity HSQC experiment gives sensitivity gains relative to the nongradient version of the same experiment as well. It is noteworthy that some of the cross peaks

(12) Cavanagh, J.; Palmer, A. G.; Wright, P. E.; Rance, M. *J. Magn. Reson.* **1991**, *91*, 429.
(13) Palmer, A. G.; Cavanagh, J.; Wright, P. E.; Rance, M. *J. Magn. Reson.* **1991**, *93*, 151.
(14) States, D. I.; Haberkorn, R. A.; Ruben, D. J. *J. Magn. Reson.* **1982**, *48*, 286.
(15) Norwood, T. J.; Boyd, J.; Campbell, I. D. *FEBS Lett.* **1989**, *2*, 369.
(16) Bax, A.; Ikura, M.; Kay, L. E.; Torchia, D. A.; Tschudin, R. *J. Magn. Reson.* **1990**, *86*, 304.
(17) Marion, D.; Ikura, M.; Tschudin, R.; Bax, A. *J. Magn. Reson.* **1989**, *85*, 393.
(18) Shaka, A. J.; Keeler, J.; Frenkiel, T.; Freeman, R. *J. Magn. Reson.* **1983**, *52*, 335.
(19) Barkhuijsen, H.; De Beer, R.; Bovee, W. M.; Van Ormondt, D. *J. Magn. Reson.* **1985**, *61*, 465.

in the new gradient experiment recorded with a single transient per FID have increased S/N relative to the corresponding peaks in the nongradient HSQC experiments (both enhanced and unenhanced) recorded with twice the number of transients. The decrease in sensitivity in the nongradient versions of the HSQC experiment is the result of presaturation applied for 1.2 s prior to the start of each scan. While the effects of presaturation on peak intensities vary, we find that for CBD presaturation attenuates the $^1H-^{15}N$ correlations on average by a factor of 1.7 relative to cross peak intensities in spectra acquired using schemes where saturation of the water resonance is avoided.

In summary, in this communication we have described a sensitivity enhanced pulsed field gradient $^1H-^{15}N$ HSQC experiment. Despite the increased number of pulses and delays over other HSQC pulse sequences, the gain in sensitivity can be significant for application to moderately sized proteins. The approach holds promise for application to a number of 3D NMR experiments such as the $^1H-^{15}N$ NOESY- and TOCSY-HSQC experiments as well as several of the triple resonance experiments.

Acknowledgment. We thank Drs. Warren, Kilburn, and Wong (University of British Columbia) for the gift of ^{15}N-labeled CBD and Drs. Guang-Yi Xu and R. Muhandiram (University of Toronto) and S. Smallcomb and S. Farmer (Varian) for useful discussions.

Supplementary Material Available: Figure illustrating a 2D contour plot of the pure absorption spectrum of CBD obtained using the sensitivity enhanced gradient sequence with one transient/FID (2 pages). Ordering information is given on any current masthead page.

C-H Insertions in the Reactions of Fischer Carbene Complexes with Ketene Acetals

Siu Ling B. Wang, Jing Su, and William D. Wulff*

Searle Chemistry Laboratory
Department of Chemistry
The University of Chicago, Chicago, Illinois 60637

Karst Hoogsteen

Biophysical Chemistry Department
Merck & Company, Inc., P.O. Box 2000, RY80M-203
Rahway, New Jersey 07065

Received August 24, 1992

In the planning of synthetic strategies that involve oxidative addition of carbon to C-H bonds, the chemical tactician could best rely on the metal-catalyzed carbenoid reactions of diazo compounds.[1,2] While these processes are commonly observed in reactions involving metal carbenoids, they are rare for stoichiometric transition metal carbene complexes, with only a single known example for the group 6 Fischer carbene complexes[3] and with the recent studies by Helquist on a group 8 complex as the only example that has been examined for synthetic utility.[4] We report the first examples of the reactions of Fischer carbene complexes with ketene acetals, which were found to stereoselectively give trans-3,4-disubstituted butanolides via a C-H insertion reaction of an in situ generated nonheteroatom-stabilized chromium carbene complex.

Scheme I

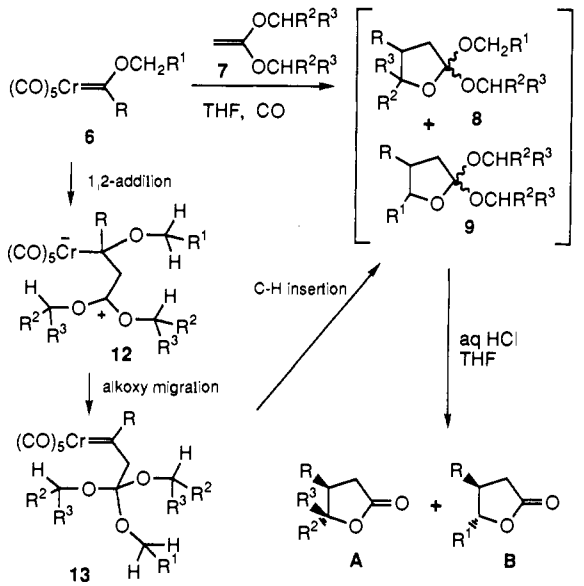

The reaction of carbene complex **1** and the ketene acetal **2** was originally performed in an effort to develop a new approach to the synthesis of cyclopropanone acetals. Although cyclopropanes can be obtained from the reactions of group 6 carbene complexes with a variety of olefins including enol ethers, the corresponding reactions with ketene acetals have never been investigated.[5,6] Surprisingly, the reaction of **1** and **2** in THF under CO did not produce any of the cyclopropanone acetal **3**, but instead produced the two isomeric tricyclic orthoesters **4** and **5** in a total of 73% yield. The stereochemistry of the major isomer **4** was determined to be that shown by an X-ray crystal structure, and the details can be found in the supplementary material.

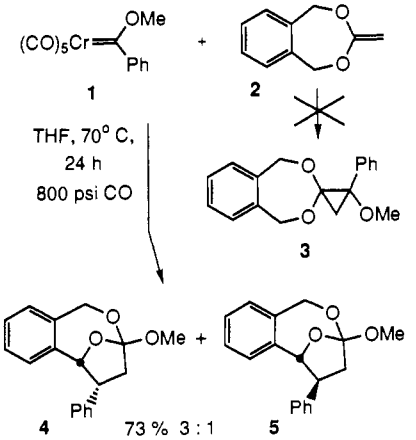

The same class of compounds was obtained from the reactions of acyclic ketene acetals as indicated in Scheme I and Table I. In this case the orthoesters **8** and **9** were not stable to silica gel and were converted to the butyrolactones **A** and **B** by treatment of the crude reaction mixture with aqueous acid during workup.

(1) For a recent review, see: Adams, J.; Spero, D. M. *Tetrahedron* **1991**, *47*, 1765.
(2) For citations to the recent literature, see: Doyle, M. P.; van Oeveren, A.; Westrum, L. J.; Protopopova, M. N.; Clayton, T. W., Jr. *J. Am. Chem. Soc.* **1991**, *113*, 8982.
(3) (a) Fischer, H.; Schmid, J.; Maerkl, R. *J. Chem. Soc., Chem. Commun.* **1985**, 573. (b) Fischer, H.; Schmid, J. *J. Mol. Catal.* **1988**, *46*, 277.
(4) (a) Zhao, S. K.; Knors, C.; Helquist, P. *J. Am. Chem. Soc.* **1989**, *111*, 8527. (b) Zhao, S. K.; Helquist, P. *J. Org. Chem.* **1990**, *55*, 5821. (c) Zhao, S.; Mehta, G.; Helquist, P. *Tetrahedron Lett.* **1991**, *32*, 5753.
(5) For reviews, see: (a) Brookhart, M.; Studabaker, W. B. *Chem. Rev.* **1987**, *87*, 411. (b) Doyle, M. P. *Chem. Rev.* **1986**, *86*, 919.
(6) For recent articles, see: (a) Harvey, D. F.; Lund, K. P. *J. Am. Chem. Soc.* **1991**, *113*, 8916. (b) Brookhart, M.; Liu, Y.; Goldman, E. W.; Timmers, D. A.; Williams, G. D. *J. Am. Chem. Soc.* **1991**, *113*, 927. (c) Brookhart, M.; Liu, Y. *J. Am. Chem. Soc.* **1991**, *113*, 939. (d) Herndon, J. W.; Tumer, S. U. *J. Org. Chem.* **1991**, *56*, 286. (e) Murray, C. K.; Yang, D. C.; Wulff, W. D. *J. Am. Chem. Soc.* **1990**, *112*, 5660. (f) Wienand, A.; Reissig, H. U. *Organometallics* **1990**, *9*, 3133. (g) Hoye, T. R.; Rehberg, G. M. *J. Am. Chem. Soc.* **1990**, *112*, 2841. (h) Soderberg, B. C.; Hegedus, L. S. *Organometallics* **1990**, *9*, 3113.

0002-7863/92/1514-10665$03.00/0